International Journal of Modern Manufacturing Technologies
ISSN 2067–3604, Vol. XI, No. 1 / 2019

EVALUATION OF COEFFICIENT OF FRICTION DURING CONICAL BENDING USING THREE ROLLER PYRAMID TYPE BENDING PROCESS

Shakil A. Kagzi[1], Harit K. Raval[2]

[1,2] Sardar Vallabhbhai National Institute of Technology
Surat, Gujarat, 395007 India

Corresponding author: Shakil A. Kagzi, shakil128@gmail.com

Abstract: Conical shells for the manufacturing of pressure vessel are generally formed using three roller pyramid type of bending process. In three roller conical bending process, the coefficient of friction (CF) between the plates and the rollers governs the power consumed during the process. It is difficult to measure the CF at the roller plate interface during bending operation. Hence, attempt has been made to evaluate the CF at the roller plate interface using bending mechanics at the top and the bottom roller. It was found that the CF varies with the bottom roller inclination but remains constant along the width of the plate. The CF at the exit side is found to be higher than at the entry side. The reported work represents the methodology of calculating CF through force mechanics, which very difficult to obtain experimentally during the bending process.

Key words: three roller bending, conical bending, friction, forces, power.

1. INTRODUCTION

Large shells of cylindrical and conical shape, used in pressure vessels industries, are generally manufactured with the help of pyramid type three roller bending process. The Figure 1 explains the pyramid type three bending process.

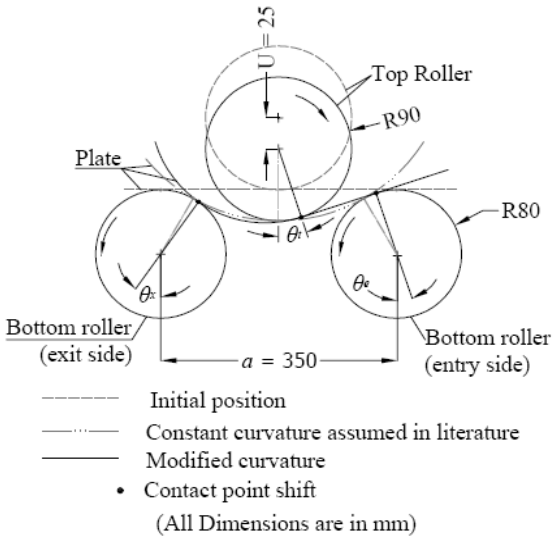

Fig. 1. Pyramid type three roller bending process (Kagzi and Raval, 2018)

This process consists of a top roller placed in middle of two bottom rollers. After placing the plate properly on the bottom roller, the top roller displacement is made towards the plate to the required distance. This movement of top roller bends the plate locally and it is defined as static bending. After the completion of the static bending, the rotational motion is provided to the bottom rollers to driving the plate for providing the curvature along the length of the plate.

The displacement of the top roller during static bending depends upon the required curvature of the plate (Gandhi and Raval, 2008; Feng and Chamliaud, 2011). For the manufacturing of the cylinder all the rollers are kept parallel. Three configuration of the roller inclination were reported by (Gandhi, 2009), for the manufacturing of the conical shell. Present study is based on one of this configuration of the conical bending in which the bottom rollers are made inclined and the top roller is made horizontal.

Based on the assumption of constant loaded radius during bending, model was reported for the prediction forces during static and dynamic conical bending by (Chudasama and Raval, 2013, 2014). The contact angles at the bottom rollers were assumed to be equal and at top roller, it was assumed to be zero. With this assumption the normal force on the top roller becomes vertical and the contact point shift during bending operation can be considered only at the bottom rollers. Moreover, the coefficient of friction (CF) at each roller plate interface was assumed to be constant.

One of the ways to overcome the assumption is through FEA simulation. A variation in curvature of the plate as well as forces during dynamic bending of the conical shell is reported by (Kagzi and Raval, 2014) through FEA simulation. (Feng et al., 2011) determined the position of lateral roll for the desired radius of cylindrical bending using FEA. (Zeng et al., 2008) maintained kinematic contact using conical roll to provide the dimensional accuracy of cone, while (Feng et al., 2009) used non-kinematic rollers. They (Feng et al., 2009) maintained accuracy by varying

CF between attachment and plate during simulation, but the CF between the roller plate interfaces was maintained constant. Use of conical rolls as well as varying CF between the attachment and the plate, as per the requirement, is practically not possible (Feng et al., 2009).

(Kagzi and Raval, 2014, 2015) reported the effect of the process parameters and material properties on forces and springback for the cylindrical and conical bending through FEA. The forces, residual strain and accuracy of the shape were investigated by (Tran et al., 2014), for asymmetrical three roller bending using experimentation and FEA. (Salem et al., 2015) discussed the forces, power and conicity for asymmetrical conical bending. In these reported simulations the CF at the roller plate interface were maintained constant.

In fact, the CF in three roller bending process at the roller plate interface depends upon the contact angles and the normal forces at the point of contact (Kagzi and Raval, 2018). Assuming the plate to be linear at entry side and having constant curvature at the exit side, CF at each roller plate interface were evaluated using mechanics of forces in case of cylindrical bending by (Kagzi and Raval, 2018).

Using simulation of three roller pyramid type bending, a flexible rolling process was introduced by (Sui et al., 2014). Using this concept of the flexible forming process as well as mechanics of forces and bending moment reported by (Kagzi and Raval, 2018), an attempt has been made to obtain the CF at each roller plate interface for one of the configurations of conical bending introduced by (Gandhi A H, 2009). Unlike the reported literature where CF is assumed to be contant during process, the present work described a mathedology to evaluate CF at each roller (top and the bottom roller) and plate interface. The CF is evaluated using mechanics of forces and the mathematical modelling, which practically very difficult to determine during the bending process.

2. EXPERIMENTATION

The experimental setup is as shown in Figure 2a, which is same setup as reported by (Kagzi and Raval, 2018) for cylindrical bending. The provision was made in experimental setup such that the span of the bottom roller can changed independently at the front and the rear side. Thus by varying the front and rear span the inclination can be provided to the bottom rollers. The Figures 2b and 2c are schematic diagram of experimental setup showing the arrangement of the rollers, load-cell and power measuring instrument. The top roller is displaced by 25mm (Figure 1) initially, and then the bottom rollers are rotated at fixed rotation speed for continues bending, to obtain curvature. The displacement of the top roller before continues bending was measured with the help of LVDT placed at the bottom of the plate (Figures 2a and 2c).

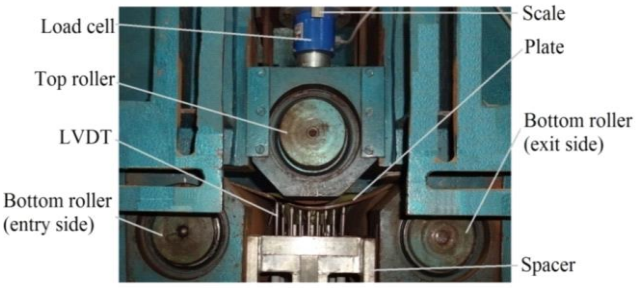

Fig. 2a. Experimental set up used for conical bending (Kagzi and Raval (2018))

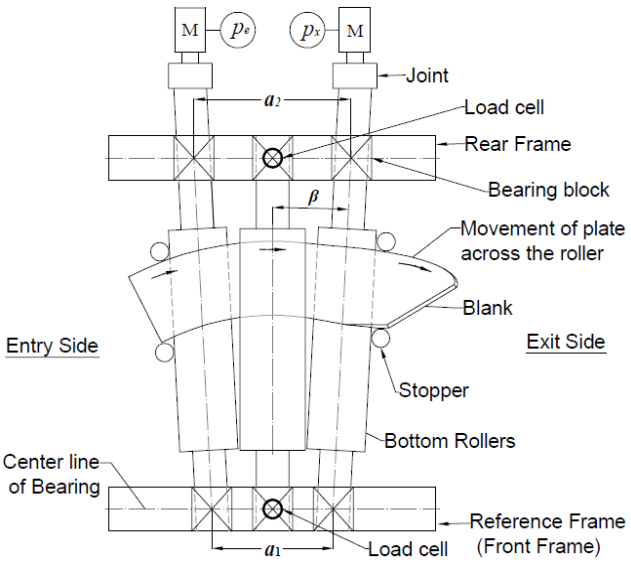

Fig. 2b. Movement of plate and experimental setup for conical bending

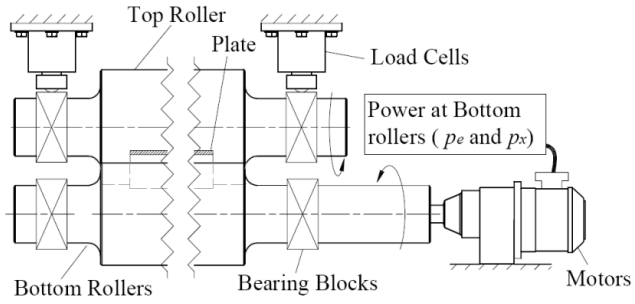

Fig. 2c. Measurement of force and power during bending (Kagzi and Raval, 2018)

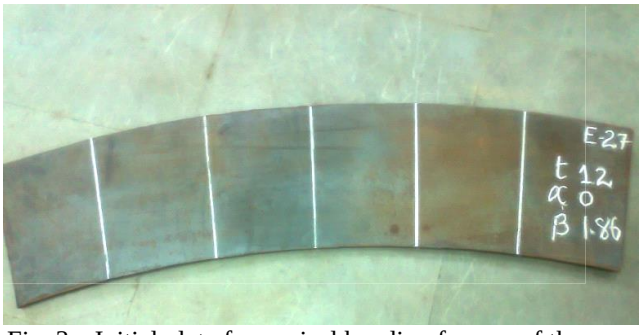

Fig. 3a. Initial plate for conical bending for one of the case (t=12mm, β=1.86°)

Fig. 3b. Plate after conical bending for one of the case (t=10mm, β=2.73°)

As per the methodology reported by (Kagzi and Raval, 2018), for the evaluation of CF at the roller plate interface an experimental force as well as the power consumption is required. Therefore, load cell was placed at the front end and the rear end of the top roller for the measurement of forces (Figure 2a and 2b). The total force on the top roller during bending will be the summation of the load obtained from both the load-cells. Both the bottom rollers (at the entry side and at the exit side of the plate) were independently connected with motor. Therefore, the power consumption of the bottom roller at the entry side (p_e) and at the exit side (p_x) can be measured during bending operation. Stoppers are placed on each side of the plate to maintain the proper movement of the plate as suggested by (Gandhi A H, 2009). Unlike the parallel rollers for the cylindrical bending reported by (Kagzi and Raval, 2018), in the present analysis the inclination provided to the bottom rollers (as shown in Figure 2b) to obtain conical bending.

The top roller is kept horizontal and the bottom roller are made inclined by fixing span (a_1) at the front side (Figures 1 and 2b) and varying span (a_2) on the rear side at the distance greater than 350 mm. Spacers are placed between the bearing blocks of the roller at front and rear end to maintain proper span (Figure 2a).

The experiments were performed considering five different levels of the bottom roller inclinations (0º, 0.37º, 0.74º, 2.71º, 3.17º), maintaining the top roller horizontal. Plates of three different thickness (8 mm, 10 mm and 12 mm) and same material grade (IS2062E300FE440) were used for experimentation. Each plate for the conical bending was cut in form of the circular segment as shown in Figure 3a. The dimensions of these circular segment were calculated using the formulation reported by (Gandhi A H, 2009), based on the roller inclination. The Figure 2a shows the conical bending being performed and bent plate after conical bending for one of the experimentation is shown in Figure 3b. During conical bending the experimental force and the power at an entry and exit side obtained and its utilization for evaluating CF is discussed in successive section.

3. MATHEMATICAL FORMULATION

For the conical bending with inclined bottom roller and horizontal top roller following assumptions were made for the evaluation of CF at the roller plate interface:

a. The width of the plate is divided in n different section.

b. For each section, the plate is assumed to be linear and tangent to the bottom roller at the entry side and the top roller.

c. At the exit side the plate is assumed to having constant curvature and tangent to top roller at the contact point and the bottom roller at the exit side (Figure 1).

d. For each section the process is assumed to be in form of cylindrical bending. Thus the bending would be uniform across the width of each section (Figure 4a). Because of the change in the span of the bottom roller along the width, the loaded radius would be different at each section.

e. The total vertical force V_t on the top roller is assumed to be varying as the combination of the uniformly distributed load and constantly varying load (Figure 4b).

f. The power across the width is assumed to be varying linearly from maximum at the front end to minimum at the rear end of the plate in the same ratio as that of the vertical top roller force in each section - equation (7).

As cylindrical bending is assumed in each section, the bending may considered to be two dimensional across the fixed width of a section of the plate. The top roller inclination is considered to be zero. Therefore, the position of the top roller at each section remains same during bending. The span between the bottom rollers at each section would be different according to the degree of the inclination of the bottom rollers. The second assumption (as discussed above) relaxes the assumption of the constant bend radius made in the literature (Feng and Champaliaud, 2011; Chudasama and Raval, 2014, 2015) and provides more realistic approach with different contact angles at each roller plate contact. Due to increase in the span of the bottom roller at each section from the front end towards the rear, the loaded radius at each section also increases. This result in decrease in the contact angles of the top and the bottom rollers across the width of the plate. The measured forces at each end can be considered to be the reaction forces on the top roller. As per the machine dimensions and the blank parameter the outer edge of the blank is kept at l_b = 600 mm from the front end of the bearing centre as shown in Figure 4b. The width of the blank was kept as w = 300 mm for all plate thickness. The length between the bearing centre of the top roller of the machine is l_r = 770 mm. As mentioned in assumption (e), if the top roller is considered to be rigid beam, the variation of the load is as shown in Figure 4b.

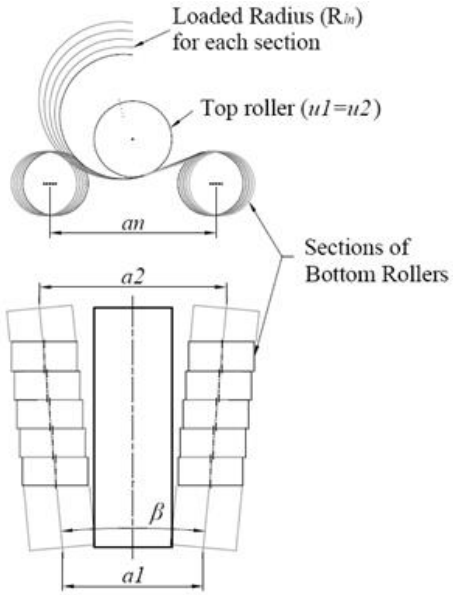

Fig. 4a. Bending along with assumed to be divided in different section

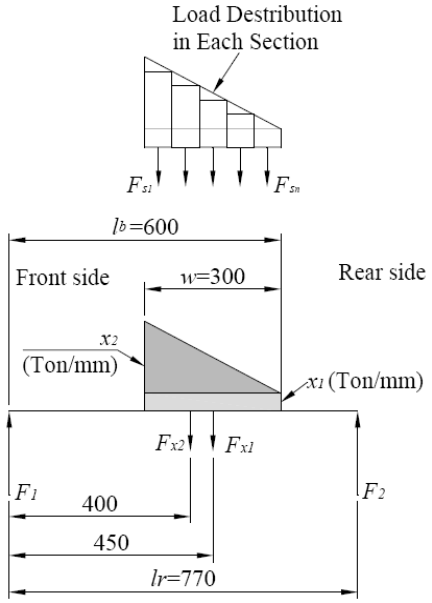

Fig. 4b. Assumed force distribution on the top roller (All dimension are in mm)

For cylindrical bending the loading condition may be assumed to uniform along the width of the plate. During conical bending, due to inclination of bottom roller the force at the front end of the plate would be more and at the rear end it would be less. This is because the radius and the span at the front end would be smaller resulting in more deformation and hence greater forces. While the span and the radius at the rear end would be more resulting in less forces. The variation of forces from front end to the rear end depends upon the extent of the bottom roller inclination. Therefore, two loading condition, namely linearly varying load and uniformly distributed load, were considered simultaneously (Figure 4b). Let x_1 be the maximum force of linearly varying load and let x_2 be the force per unit length for uniform distributed load. Let F_{x1} and F_{x2} be the resultant force due to uniformly distributed load and uniformly varying load. Therefore, these resultant forces may be defined as shown in equations (1) and (2).

$$F_{x1} = (x_1 \cdot w) \tag{1}$$

$$F_{x2} = (0.5 \cdot x_2 \cdot w) \tag{2}$$

Let F_1 and F_2 be the forces measured by the load cell at the front and the rear end respectively. Balancing the vertical forces and the moment about the bearing centre at the front end, equations (3) and (4) holds well. In both of these equations unknown parameters are x_1 and x_2. Hence, these two equations can be solved for obtaining x_1 and x_2.

$$F_{x_1} + F_{x_2} = F_1 + F_2 = V_1 \tag{3}$$

$$-(F_2 \cdot l_r) + \left(F_{x_2} \cdot \left(l_b - \frac{2w}{3}\right)\right) + \left(F_{x_1} \cdot \left(l_b - \frac{w}{2}\right)\right) = 0 \tag{4}$$

The value of the vertical force in each section (F_{sn}) can be calculated using x_1 and x_2. Let, tan (d) is the slope of the uniform varying load, the width of the plate is divided into sections of equal width (w_s), F_{s1}... F_{sn} be the vertical force in the respective section. Then the value of the vertical reaction forces in each section is given by,

$$F_{s1} = ((x_2 - 0) \cdot w_s) - (0.5 \cdot w_s \cdot (w_s \cdot \tan d)) + (x_1 \cdot w_s)$$

$$F_{s2} = ((x_2 - [1 \cdot w_s \cdot \tan d]) \cdot w_s) - (0.5 \cdot w_s^2 \cdot \tan d) + (x_1 \cdot w_s)$$

Generalising the above equations of vertical force for the nth section we have equation (5),

$$F_{sn} = ((x_2 - [(n-1) \cdot w_s \cdot \tan d]) \cdot w_s) - (0.5 \cdot w_s^2 \cdot \tan d) + (x_1 \cdot w_s) \tag{5}$$

As per the assumption (f), the power varies in a same slope as that of vertical bending force. Therefore, the following relation holds good.

$$\frac{P_{en}}{P_e} = \frac{F_{sn}}{V_t} \tag{6}$$

$$\frac{P_{xn}}{P_x} = \frac{F_{sn}}{V_t} \tag{7}$$

Thus for each section of the plate (along width), the force as well as power consumption can be calculated. As the bending at each section is assumed to be cylindrical. The evaluation of CF can be done independently and iteratively at each section along the width of the plate as explained (Kagzi and Raval, 2018). Thus the values of these forces and power at each section are used to evaluate the CF at each roller plate interface using the mathematical model and algorithm reported by (Kagzi and Raval, 2018). The experimental results and the CF evaluated at the roller plate interface are discussed in successive section.

4. RESULTS AND DISCUSSION

The experiments of conical bending were performed with different bottom roller inclination and three different plate thicknesses as discussed in previous section. The rotation of the bottom rolls causes the plate to move across the rollers continuously and thus the continuous bending take place. During continuous bending the measured average force (F_d) with respect to bottom roller inclination as shown in Figure 5. This graph is plotted for different plate thickness. The numeral following '*t*' indicates thickness. It is seen that the increase in thickness results in increase in the bending force. This is due to increase in strength of plate with respect to thickness. The dotted trend line shows the decrease in force with increase in the bottom roller inclination. The span along the width increases with the increase in the bottom roller inclination. Therefore, the loaded radius increases resulting in reduction in load.

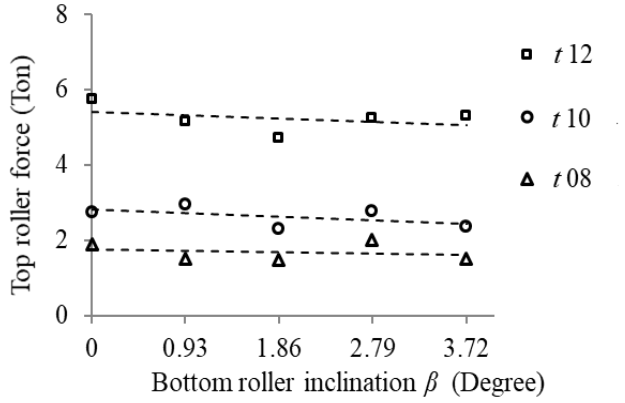

Fig. 5. The forces measured at the top roller during continuous bending process

The average power consumption measured at the entry and the exit side during continues bending operation with respect to bottom roller inclination is as shown in Figure 6. The continuous and the dotted lines are the trend line for the power consumed at the bottom roller of the entry side and the exit side respectively. It is seen that the power at the entry side is higher than the power at the exit side. As the top roller is driven by the bottom roller at the entry side and mostly the bending take place at the entry side, the power consumed at entry side is higher than at exit side. Smaller variation in power is found with respect to the bottom roller inclination. It is also seen that the increase in the thickness requires greater power for the continuous bending process. The strength of the plate and hence the normal force at the bottom roller increases with increase in the thickness of the plate. These increase in the power with respect to thickness of plate.

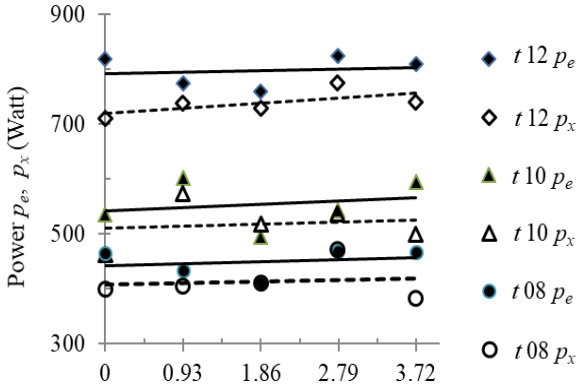

Fig. 6. The power measured during continuous bending process

Thus the total force at the top roller and the power consumption at the bottom rollers were experimentally obtained. The width of the plate during conical bending was assumed to be divided in different sections (Figure 4a). Assuming the linear variation of the forces and power across the width of the plate the forces and the power consumption at each section was determined - equations (1)-(5). Force and power obtained for perticular section was used to calculate CF at each roller plate interface at that section.

For the conical bending it is required to determine the number of section across the width of the plate. The variation in the results was found to be very small when the number of section along width was increased beyond five. Therefore, the width (w = 300 mm) of the plate in present case was divided in five sections. Each section was having the width of w_s = 60 mm. The results were obtained for different plate thickness and bottom roller inclinations.

The variation of forces at the roller plate interface, evaluated across the width of the plate is as shown in Figure 7 for one of the experimentation (t = 10 mm, β = 1.86˚, α = 0˚). Due to assumption of the bending force and power explained in the earlier section (equations (6) and (7)), the variation of the normal forces at the bottom roller along the width of the plate, is found to be linear. Also it is found that the normal forces at the exit side to be less than that at the entry

side. The reason is similar as that explained earlier for the power consumed at entry and exit side. Similar linear variations of the normal forces were observed for each bottom roller inclination. The total normal force acting at each bottom roller may be considered to be the summation of the forces exerted at each section. Thus the normal forces at the bottom roller on the entry side and that at the exit side for different thickness and bottom roller inclination is shown in Figures 8a and 8b respectively. The normal forces are found to be increasing with increase in the thickness of the plate. It can be seen that the normal force at the bottom rollers appears to be decreasing with increase in the bottom roller inclination (Figures 8a and 8b).

The Figure 8c shows the variation in the CF along the width of the plate for one of the roller configuration. It is seen that the CF along the width of the plate is almost constant in spite of the linear variation in the normal forces. Similarly, for the each configuration of bottom roller inclination the CF was found to be almost constant along the width of the plate (for each section). Hence, CF for each roller inclination was considered to be the average value of the CF obtained along the width of the plate. The variation of CF at the bottom roller on the entry as well as exit side is as shown in Figures 9a - 9c for the thickness of 12 mm, 10 mm and 8 mm respectively.

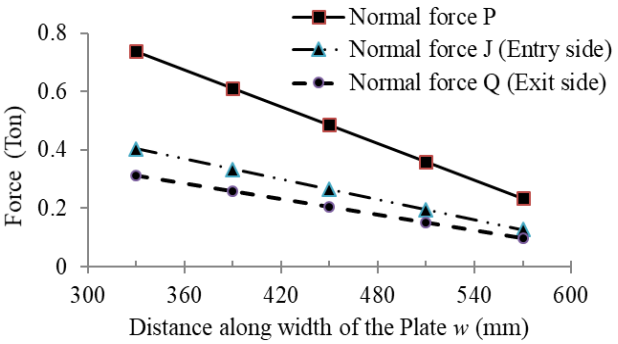

Fig. 7. Normal Forces along the width of plate at each roller-plate interface (t=10, β=1.86˚, α=0˚)

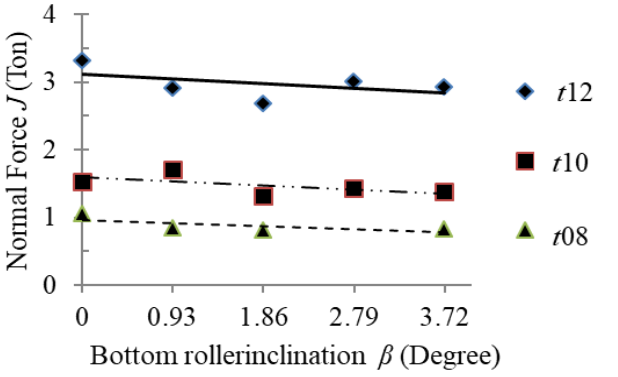

Fig. 8a. Total normal force (J) for different bottom roller inclination β and thickness t (α=0˚)

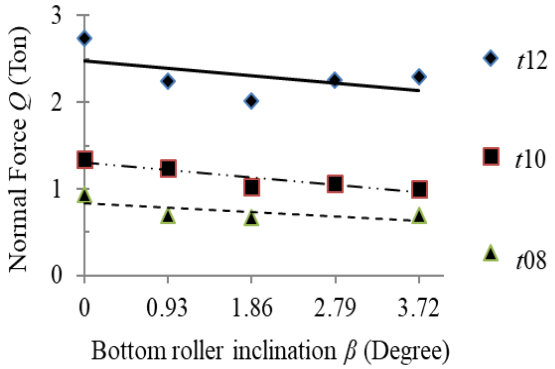

Fig. 8b. Total normal force (Q) for different bottom roller inclination β and thickness t (α=0˚)

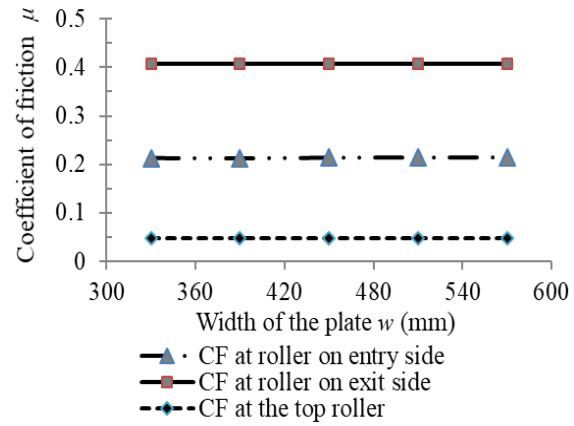

Fig. 8.c. CF obtained along the plate width for (t=10mm, β=1.86˚, α=0˚)

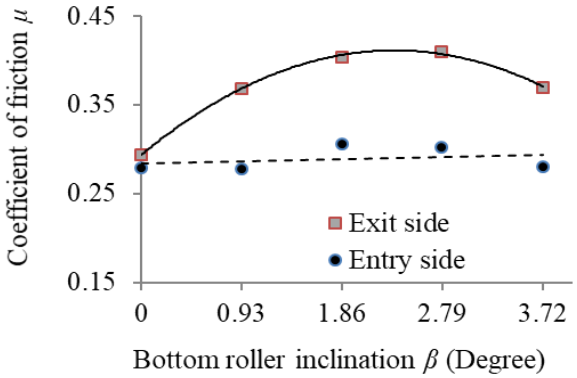

Fig. 9a. CF on entry and exit side versus β (t=12mm, α=0º)

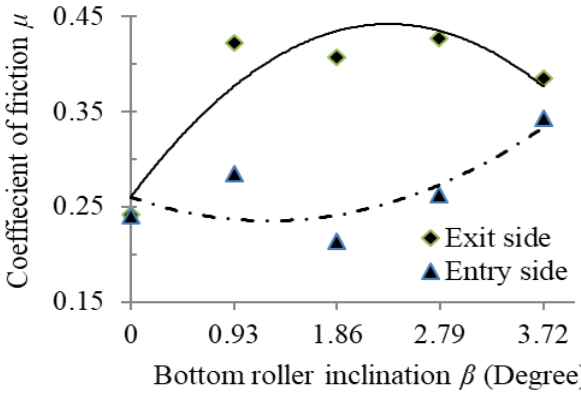

Fig. 9b. CF on entry and exit side versus β (t=10mm, α=0º)

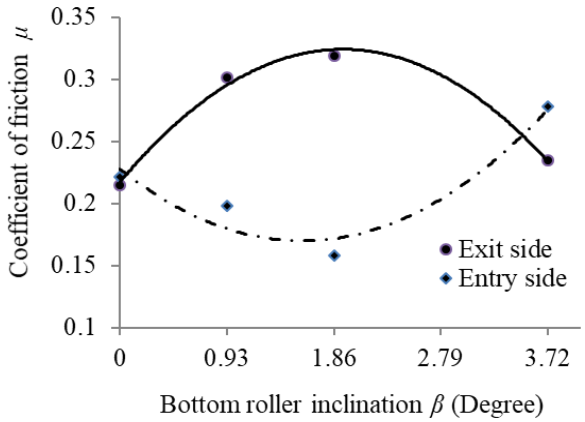

Fig. 9c. CF on entry and exit side versus β (t=8mm, α=0º)

The CF at the bottom rollers are under the effect two conditions with increase in β, namely, decrease in contact angle (which decreases CF) and decrease in normal forces (which increases CF). The CF at the entry side is found to varying non-linearly with bottom roller inclination for the lower thickness (8 mm, Figure 9c). This non-linearity decreases with increase in thickness of the plate. It is seen that the mean curve fitted for CF at the entry side decreases to minimum and then onwards it increases for the thickness of 8 mm and 10 mm with increase in bottom roller inclination. At the entry side the frictional force supports the vertical bending force at the top roller and the contact angle decreases with increase in span of the bottom rollers. Therefore, CF decreases to an extent with increase in bottom roller inclination. For all the thickness the CF at exit side varies non-linearly with β. Towards the exit side the contact angle is higher than that at the entry side. Also the normal force acting of the bottom roller at the exit is found to be lower than at the entry side. In case of conical bending with bottom roller inclination, the CF at the exit side is found to be higher than at the entry side. It is seen that for all the three cases the maximum CF occurs in between β = 1.86˚ and 2.79˚.

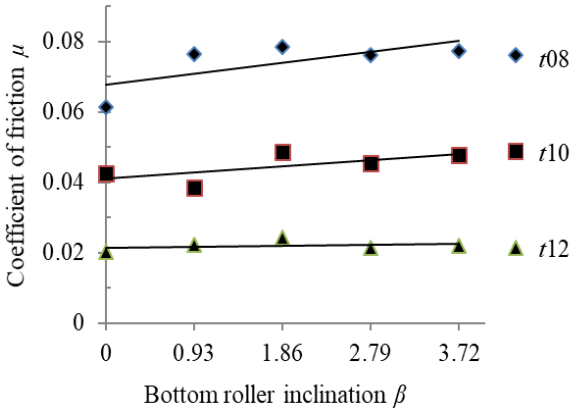

Fig. 10. CF at top roller versus β (α=0º)

The CF at the top roller and plate interface calculated is plotted in Figure 10. From the trend drawn passing through the plotted points it is seen that the CF varies almost linearly with β. The variation is more in 8 mm thickness and it decreases with thickness of the plate. The CF of 12 mm thickness is almost found to be constant. CF is also found to be decreasing with increase in the thickness of the plate.

In conical bending with the increase in the bottom roller inclination, the reaction forces at the top roller decreases. Therefore, the CF at the top roller interface increases to drive the plate without slip. The CF at the top roller interface is found to be lower than bottom roller interface.

5. CONCLUSION

A model has been reported for finding coefficient of friction between roller plate interfaces in three roller conical bending. The model reported was based one of the roller configuration of conical bending which includes bottom roller inclination and horizontal top roller.

The experimentations were performed and coefficient of friction was evaluated with the help of model reported in the literature and an experimental data. With increase in the bottom roller inclination the CF increases to an extent and then decreases. Along the width of the plate the CF remains constant in conical bending although the normal forces at each roller plate interfaces is found to decreases from the side of the smaller radius to that towards the side of higher radius. The derived mathematical modelling is helpful in finding out the coefficient of friction for the bottom roller inclination, which is very difficult to find out practically under actual condition.

6. ACKNOWLEDGEMENTS

Authors appreciate and acknowledge the valuable support and the funding provided by the Department of Science and Technology (DST), Ministry of Technology, Government of India as the present work is a part of project sponsored by the DST [Grant sanction number: SR/S3/MERC-0047/2011 dated: 16/04/2012].

7. NOMENCLATURES

a_1, a_2 Span of the bottom rollers at the front and rear side

F_1, F_2 Vertical force measured at the front and the rear end of the top roller

F_{x1}, F_{x2} ... F_{xn} Resultant force due to uniformly distributed load and uniformly varying load respectively

F_{s1}, F_{s2} ... F_{sn} Resultant vertical force at each section.

J Normal force at the contact between the plate and the bottom roller at the entry side

n number of section along the width of the plate

P Normal force at the top roller contact point
p_e, p_x Power consumed during bending at the bottom roller at the entry and the bottom roller on the exit side respectively
p_{en}, p_{xn} Power consumed during bending at the bottom roller at the entry and the bottom roller on the exit side respectively at n^{th} section
Q Normal force at the contact between the plate and the bottom roller at the exit side
t Thickness of the plate
U Displacement of the top roller
V_t Total vertical force on the top roller
w Width of the plate
x_1, x_2 Maximum force per unit length
μ Friction coefficient (CF)
θ_t, θ_e, θ_x Contact angle at the top roller, the bottom roller at the entry and the bottom roller on the exit side respectively
α Top roller inclination angle in degree
β Bottom roller inclination angle in degree

8. REFERENCES

1. Gandhi, A.H., Raval, H.K., (2008). *Analytical and empirical modelling of top roller position for three roller cylindrical bending of plates and its experimental verification*. Journal of material processing technology, 197(1-3), 268-278.
2. Feng, Z., Chamliaud, H., (2011). *Modelling and simulation of asymmetrical three-roll bending process*. Simulation Modelling Practice and Theory, 19(9), 1913-1917.
3. Gandhi, A.H., (2009). *Investigation on Machine Setting Parameters for 3-Roller Conical Bending Machine for Springback*. PhD thesis, S. V. National Institute of Technology, Surat, Gujarat, India.
4. Chudasama, M.K., Raval, H.K., (2013). *An approximate bending force prediction for three roller conical bending process*. Journals of materials forming, 6(2), 303-14.
5. Chudasama, M.K., Raval, H.K., (2014). *Bending force prediction for dynamic roll-bending during 3-roller conical bending process*. Journal of Manufacturing processes, 16(2), 184-295.
6. Kagzi, S.A., Raval, H.K., (2014). *An Investigation of forces during roller forming process*. Advanced Materials Research, 1036, 337-343.
7. Zeng, J., Zhao, Heng, L., Chamliaud H., (2008). *FEM dynamic simulation and analysis of roll-bending process for forming of conical tube*. Journal of material processing technology, 198(1(3)), 330-43.
8. Feng, Z., Chamliaud, H., Dao, Thien-My, (2009). *Numerical study of non-kinematic roll bending process with conical rolls*. Simulation Modelling Practice and Theory, 17(10), 1710-1722.
9. Kagzi, S.A., Raval, H.K., (2015). *An Analysis of Forces during Three Roller Bending Process*. International Journal of Materials and Product Technology, 51(3), 248-263.
10. Tran, Q.H., Champliaud, H., Feng, Z., Dao, T.M., (2014). *Analysis of the asymmetrical roll bending process through dynamic FE simulations and experimental study*. International Journal of Advanced Manufacturing Technology, 75(5-8), 1233–1244.
11. Salem, J., Champliaud, H., Feng, Z., Dao, Thien-My, (2015). *Experimental analysis of an asymmetrical three-roll bending process*. International Journal of Advanced Manufacturing Technology, 83(9-12), 1823-1833.
12. Kagzi, S.A., Raval, H.K., (2018). *Forces and coefficient of friction during cylindrical three roller bending*. Journal of the Brazilian Society of Mechanical Sciences and Engineering, 40, 129.
13. Sui, Z., Cai, Z., Lan, Y., Liu L., (2014). *Simulation and software design of continuous flexible roll bending process for three dimensional surface parts*. Materials and Design, 54, 498-506.
14. Indian Standards (2006) IS2062: *Hot rolled medium and high tensile structural steels*, New Delhi: Bureau of Indian Standards.

Received: December 10, 2018 / Accepted: June 15, 2019 / Paper available online: June 20, 2019